ELSEVIER

Journal of Nuclear Materials 313–316 (2003) 888–892

journal of nuclear materials

www.elsevier.com/locate/jnucmat

Two-dimensional distribution of divertor radiation in JT-60U

S. Konoshima *, H. Tamai, Y. Miura, S. Higashijima, H. Kubo, S. Sakurai, K. Shimizu, T. Takizuka, Y. Koide, T. Hatae, H. Takenaga

Japan Atomic Energy Research Institute, 801-1 Mukouyama, Naka-machi, Naka-gun, Ibaraki-ken 311-0193, Japan

Abstract

Two-dimensional (2D) reconstruction software was developed for bolometer signals of the JT-60U tokamak. Radiative divertor plasma with emissivity of 10 $MW\,m^{-3}$ was found previously to extend 10 cm from the target plates. When the density is increased further by larger gas puffing, the emissivity imbalance between both divertor legs becomes less significant. The radiative zones move upward along the divertor legs and eventually merge into a single bright peak near the X-point at density around 6×10^{19} m^{-3} called X-point multifaceted asymmetric radiation from edge. Upward movement of the radiation peak during detachment is sometimes observed directly by the in-vessel bolometer. Total radiated power at the divertor saturates at a certain level while the core radiation continues to increase with the density. Although the 2D profile of the divertor radiation undergoes dramatic changes near the saturation, the energy confinement appears to degrade with density increase irrespective of these changes.

PACS: 52.55.Fa
Keywords: Tokamak; Divertor plasma; Radiation loss; 2D tomographic reconstruction; Power balance; MARFE

1. Introduction

Radiative divertor operations with gas puffing have been studied searching possible solutions to reduce heat load on the divertor target plate and to achieve high density plasmas favorable for a fusion reactor. Understanding complex space–time structures of divertor radiation, which is a kind of self-organization process, has been an active area of investigation. Software for the two-dimensional (2D) reconstruction of bolometry [1] has been developed for the JT-60U tokamak and signals of a 48-channel bolometer system have made it possible to be mapped onto the divertor geometry [2]. Reconstructed 2D radiation profiles provide an intuitive understanding of experiments and comparison with simulation for divertor characterization. High density and low temperature plasmas in most of the divertor volume have been explored previously [3]. Energy confinement of H-mode plasmas is known to degrade at high densities below the Greenwald density in most of the tokamaks including JT-60U [4], except a certain class of high density discharges in DIII-D [5]. In this paper we will present 2D divertor radiation characteristics of high-density discharges and some discussions in comparison with argon seeded discharges. The direction of the ion grad-B drift is towards the divertor in this study.

The JT-60U bolometer system consists of four large cameras installed in the diagnostic ports with a total of 32 viewing chords and four small in-vessel cameras with 4 viewing chords each. Divertor cameras have much better spatial resolution and it is their profile that drives much of the structure in the 2D reconstruction. In order to obtain the distribution of local emissivity in the poloidal cross section, measured line integrals must be unfolded. The core radiation profile is determined separately by so-called Abel inversion with signals which view only the core plasma, assuming emissivity is

* Corresponding author. Tel.: +81-29 270 7612; fax: +81-29 270 7419.
E-mail address: konoshis@fusion.naka.jaeri.go.jp (S. Konoshima).

0022-3115/03/$ - see front matter © 2003 Elsevier Science B.V. All rights reserved.
PII: S0022-3115(02)01471-X

uniform along magnetic flux surface. Divertor radiation is analyzed as a remaining part of the signals. The 2D distribution of the divertor radiation is obtained as a least squares solution of linear equations for the unknown emission of more than 1000 cells with a response matrix of the view chords. A smoothing constraint is applied additionally to regularize the solution with a form of diffusive process. Details of the formalism and methodology of inversion including bolometer hardware are described in Ref. [2].

2. Evolution of 2D divertor radiation profile

2.1. High density discharge with deuterium gas fuelling

An example of high density discharges with a large deuterium gas puffing in the JT-60U tokamak is shown in Fig. 1(a). Line average density n_e rises to 98% of the Greenwald density, $n_{GW}[10^{20}\ \mathrm{m}^{-3}] = I_p\ [\mathrm{MA}]/(\pi a^2\ [\mathrm{m}])$ [6], in response to 150 Pa m^3/s of deuterium gas puff. Two interferometer signals at $r/a \sim 2/3$ of inboard (solid line) and $r/a \sim 1/3$ of outboard side (dashed line) are fully overlapped like a single line indicating a flat density profile. Large gas fueling normally leads to a loss of the energy confinement during density rise seen in the stored energy W_{dia}. The H-factor relative to L-mode (89 power law scaling) is low around 1 (cf. Fig. 4). The edge localized mode (ELM) activity observed in the D_α signal, thought to be a type III ELMs, becomes smaller near the maximum of density. Total radiative power from the core plasma P_r^{core} increase with the density, while the divertor radiative power P_r^{div} shows a roll over at some point. Evolution of 2D divertor radiation profiles at time slices shown by the dashed lines in (a) are displayed in Fig. 1(b). The contours of the radiation peaks are shown in linear scale up to 20 MW/m^3 together with constant emissivity lines of 5 and 10 MW/m^3, two dashed contours. Immediately after the large gas puffing and the main heating are applied, there appear two symmetric radiation peaks at inboard and outboard strike points with almost equal emissivity at 7 s. At 7.5 s , the inboard radiation peak moves upstream to a half way point and the outboard radiation starts spreading toward the X-point. A redistributed radiation profile extends the whole divertor region uniformly without having any peaks at 8 s and starts a contraction into a bright spot near the X-point at 8.5 s. The line average density is $5.2 \times 10^{19}\ \mathrm{m}^{-3}$, or 83% of n_{GW} at this stage. Radiation condensation, or so-called X-point multifaceted asymmetric radiation from edge (MARFE) [7], is formed and kept stationary near the X-point in the final stage during 9–10 s. No radiation is observed near the target plate indicating the divertor plasma is detached fully from the walls. The diameter of a half-maximum of the peak is about 10 cm with an

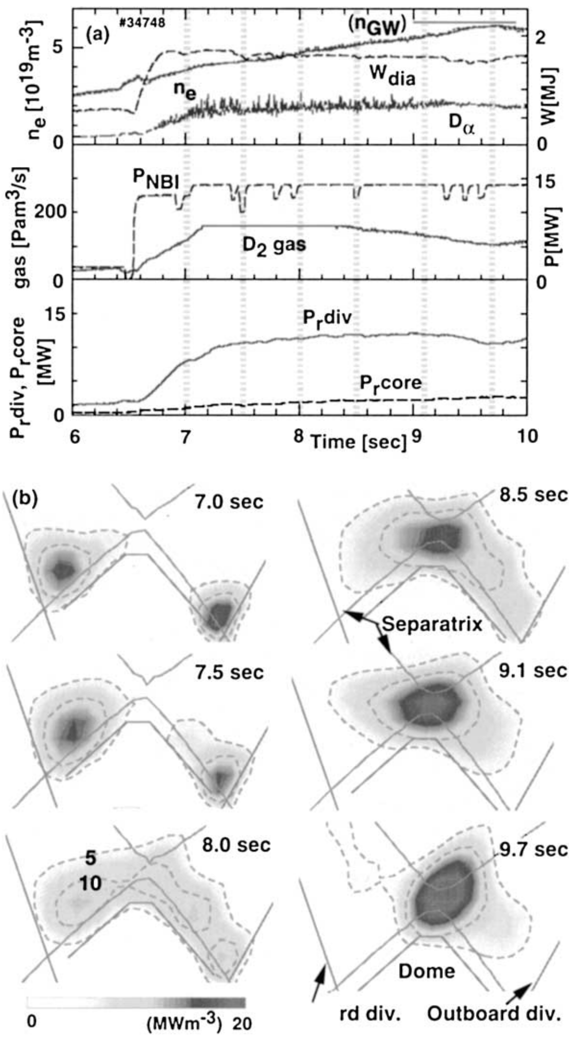

Fig. 1. (a) High density discharge with D_2 gas puffing and beam heating P_{NBI}. Toroidal field B_t and plasma current I_p are 3.6 T and 1.4 MA, respectively. (b) 2D divertor radiation profiles at times shown dashed lines in (a). Two emissivity contour lines are 5 and 10 MW m^{-3}.

emissivity more than 20 MW/m^3. In–out symmetry of the peak emissivity is a characteristic of heavy gas puffing discharges. This is in marked contrast to the medium density discharges, $3–4 \times 10^{19}\ \mathrm{m}^{-3}$, reported earlier (Figs. 7 and 8 of Ref. [2]), in which the outboard emissivity was a factor 2–3 smaller. The outboard divertor radiation rises earlier responding to the gas puff than the signals of other chords in high density discharges. A rapid rise of the bolometer signal is sometimes found to be due to a possible response to charge exchange neutrals [8,9]. Larger radiation at the outboard strike point in an early stage appears to suggest an increase of charge exchange neutrals associated with heavy gas fueling.

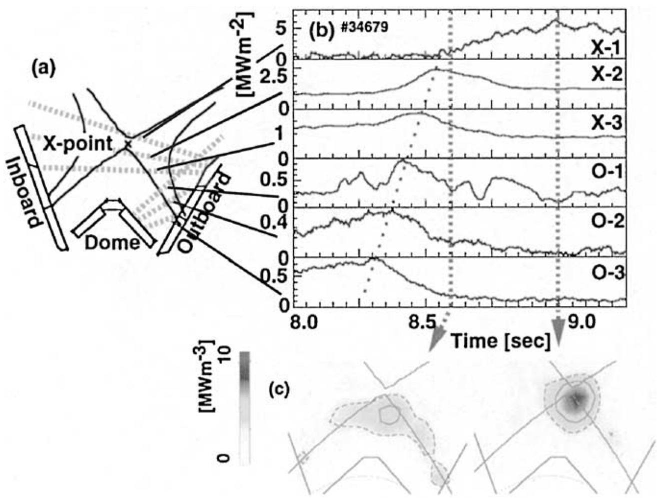

Fig. 2. (a) Viewing chords of the camera (- - -) and the divertor geometry. (b) Bolometer signals monitor upward movement of radiation peak. (c) 2D radiation profiles showing subsequent radiation condensation near the X-point. Dashed and solid lines are 3 and 5 MW m^{-3}, respectively. $I_p = 1.2$ MA and $B_t = 3.5$ T.

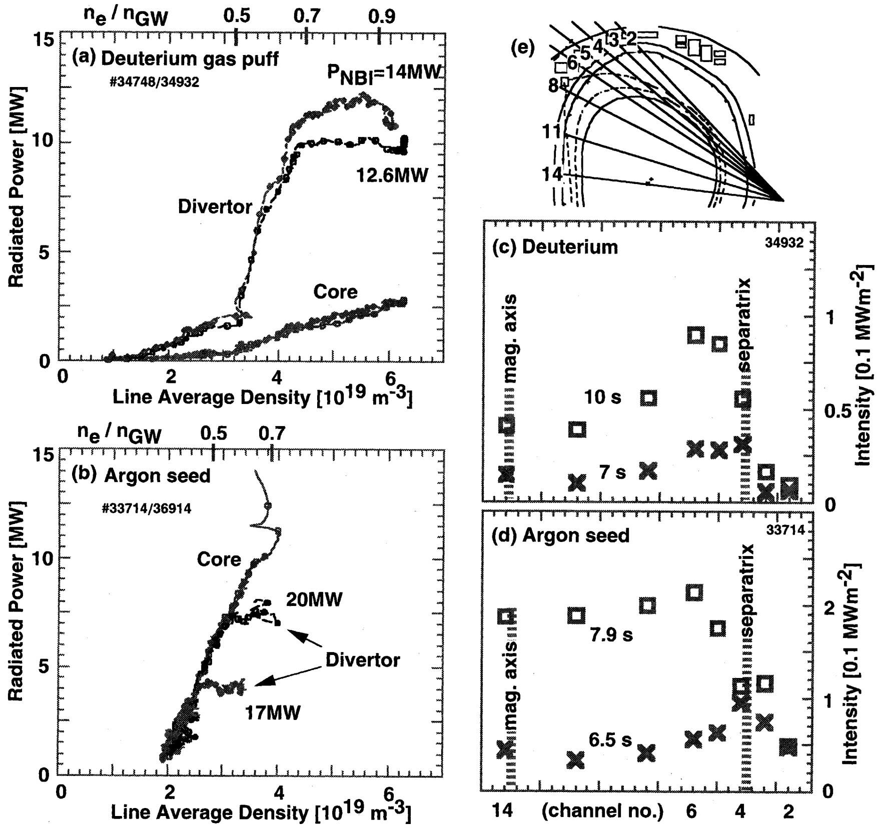

Fig. 3. Trajectories of total radiated power from divertor and core for D_2 gas fuelled (a) and argon seeded discharges (b) as a function of the density. (a) $I_p = 1.4$ MA, $B_t = 3.6$ T and (b) $I_p = 1.2$ MA, $B_t = 2.5$ T. Line integrated core radiation profiles (□) of D_2 (c) and argon seeding (d) are compared with profiles just before D_2 or argon puff application (×), (e) channel numbers.

2.2. Movement of radiation peak during detachment

The divertor bolometer camera sometimes records upward movement of a radiation peak during the process of detachment. The camera monitors several points along divertor leg as shown in Fig. 2(a). The discharge is a low beam power L-mode of 4 MW with a relatively large D_2 gas puffing rate of 15 Pa m^{3}s^{-1}. Signals of relevant channels are displayed in Fig. 2(b). The start of the detachment is identified as a drop of the O-3 signal viewing the outboard strike point at 8.3 s. Divertor Langmuir probes indicated that detachment started at around 8.3 s with a time resolution of 0.1 s both from inboard and outboard strike points (not shown). The line average density is 1.8×10^{19} m^{-3} or 40% of n_{GW} at this moment. Following this drop, upward movement of radiation peak is seen successively in upstream channels towards X-point, O-2 $\sim$ X-2, although X-2 and X-3 include another peak coming from the inboard side. The radiation peak travels from the target tile to the X-point in 0.3 s which corresponds to a poloidal velocity of about 0.8 m/s. The next step, formation of X-point MARFE, takes another 0.4 s, as shown by 2D radiation profiles [10] at two time slices in Fig. 2(c). The radiation condensation can be a slow process. A broad emission profile of a crescent shape centered near the X-point turns to a circular MARFE with a time scale longer than that of the energy confinement. No appreciable changes of the divertor neutral pressure [11] were identified for this particular case. This may be partly due to relative insensitivity of the pressure signal as a direct particle source because of a short mean free path [12].

3. Saturation of the divertor radiation

It is usually observed in JT-60U radiative divertor experiments that the total radiated power from the core plasma P_r^{core} increases linearly with the density, while the divertor radiation P_r^{div} appears to saturate at some point of the density, as in the example shown in Fig. 1. Saturation is observed also during argon seeding experiments. The trend is seen clearly in Fig. 3 in which evolutions of total radiation power are plotted as a function of line average density. Fig. 3(a) and (b) compares typical evolutions of radiated power for deuterium gas fuelled and argon seeded discharges. Normalized density to the Greenwald density, n_e/n_{GW}, is shown in the top. Argon contamination are estimated 0.7–1% of the electron density at $\sim 3 \times 10^{19}$ m^{-3} [13,14]. The two discharges in Fig. 3(a) and (b) are almost identical other than a small difference in heating power. Heating and gas puffing are applied at a density of 3.2×10^{19} m^{-3} in (a) and 2×10^{19} m^{-3} in (b). Deuterium fuelling shows a faster rate of rise of the divertor radiation than the core radiation, while argon seeded shots are characterized by a rapid increase of the core radiation similar to the divertor radiation. A faster rise of the divertor radiation than that of the core in (a) is thought primarily due to the larger cooling rate of carbon at a few tens of eV than that above 1 keV of the core plasma in addition to the possible contribution of charge exchange loss. A large cooling rate of argon is thought responsible for rapid increase of core radiation in (b). A significant increase over the whole radius in the argon seeded case, while the radiation increase was limited only at the edge in the case of deuterium, are displayed in Fig. 3(c) and (d). A small peak outside the separatrix in (d), ch3, is associated with a 2nd separatrix which has a null point outside the top vessel walls. Frequency decrease of ELMs and sawtooth also contributes some of the enhancement of core radiation.

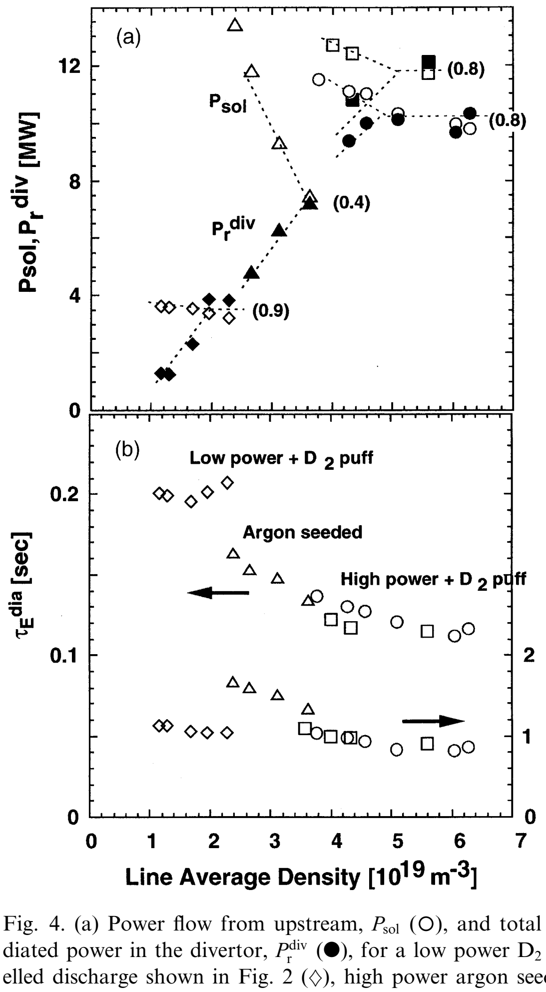

Fig. 4. (a) Power flow from upstream, P_{sol} (○), and total radiated power in the divertor, P_r^{div} (●), for a low power D_2 fuelled discharge shown in Fig. 2 (◇), high power argon seeded shot (Fig. 9 of Ref. [2]) (△) and two high power discharges fuelled with large D_2 gas puff shown in Fig. 3 (a) (○ and □). Numbers are ratios of saturated radiation power to the heating power. (b) Energy confinement time and H-factor relative to L-mode scaling.

The saturation of the divertor radiation is found to occur whenever the power flow from the core plasma, P_{sol}, is approximately equal to the radiated power at the divertor, as plotted in Fig. 4(a). Here P_{sol} $(= P_{NBI} - P_r^{core})$ is defined as a remaining power which has not been dissipated by the core radiation. The P_{sol} is a fraction of power to be transferred to the divertor through the scrape off layer by conductive and/or convective transport from the core to the divertor. Several time slices of four different discharges are displayed. These includes low power with gas puffing discharge shown in Fig. 2 (diamonds), high power argon seeded shot (Fig. 9 of Ref. [2]) (triangles) and two high power and high density discharges shown in Fig. 3(a) and 1 (circles and squares). The saturated power corresponds about 80–90% of the injected power for deuterium gas puff, while in the case of argon the saturation occurs at around 40% of the input power due to a large radiative dissipation in the core. Fig. 4(b) shows the energy confinement time measured with diamagnetism τ_E^{dia} and the H-factor relative to L-mode scaling for the same discharges. The confinement time appears to decrease inversely proportional to the density except low power shot, irrespective of the changes in (a). On the other hand, the normalized confinement, H-factor, of these discharges other than argon seeded shots are shown to be nearly 1, despite the differences in the plasmas. High pedestal temperature preserving profile stiffness was reported as a reason for the confinement improvement of argon seeded discharges [13–15].

4. Summary

Evolution of 2D divertor radiation profiles during deuterium gas puffing has been analyzed. In–out symmetric radiation localized at the target, redistributes to a uniform profile along divertor legs and evolves into a single peak condensed near the X-point, MARFE. Movement of radiation peak during the detachment process is possible to observe directly by the divertor bolometer that might be useful for divertor control. Deuterium fuelling gives a faster rate of rise of the divertor radiation relative to the core, while argon seeded shots are characterized by a large increase of the core radiation which results in early saturation of the divertor radiation. Although 2D profiles of the divertor radiation undergoes dramatic changes during saturation, the energy confinement appears to degrade simply due to the density increase by deuterium gas puffing irrespective of the changes in divertor radiation.

References

[1] A.W. Leonard et al., Rev. Sci. Instrum. 66 (2) (1995) 1201.
[2] S. Konoshima et al., Plasma Phys. Control. Fusion 43 (2001) 959.
[3] M.E. Fenstermacher et al., Phys. Plasmas 4 (5) (1997) 1761.
[4] N. Asakura et al., J. Nucl. Mater. 266–269 (1999) 182.
[5] T.H. Osborne et al., J. Nucl. Mater. 290–293 (2001) 1013.
[6] M. Greenwald et al., Nucl. Fusion 28 (1988) 2199.
[7] D.R. Baker et al., Nucl. Fusion 22 (1982) 807.
[8] N. Hosogane et al., Nucl. Fusion 34 (1994) 527.
[9] R. Reichle et al., J. Nucl. Mater. 241–243 (1997) 456.
[10] T. Sugie et al., Fusion Sci. Technol. 42 (2002) 482.
[11] H. Tamai et al., Proceedings of the 26th EPS Conference on Controlled Fusion and Plasma Physics, June 1999, Maastricht.
[12] R.L. Boivin et al., Phys. Plasmas 7 (2000) 1919.
[13] S. Sakurai et al., J. Nucl. Mater. 290–293 (2001) 1002.
[14] H. Kubo et al., Nucl. Fusion 41 (2001) 227.
[15] J. Ongena et al., Plasma Phys. Control. Fusion 43 (2001) A11.